

# Compact MEMS Mirror Based Q-Switch Module for Pulse-on-demand Laser Range Finders

Veljko Milanovic, Abhishek Kasturi, Bryan Atwood, Yu Su, Kevin Limkrailassiri  
Mirrorcle Technologies, Inc., Richmond, CA  
John E. Nettleton, Lew Goldberg, Brian J. Cole  
US ARMY Night Vision & Electronic Sensors Directorate, Fort Belvoir, VA  
Nathaniel Hough, Fibertek, Inc., Fort Belvoir, VA

## ABSTRACT

A highly compact and low power consuming Q-switch module was developed based on a fast single-axis MEMS mirror, for use in eye-safe battery-powered laser range finders. The module's 1.6mm x 1.6mm mirror has >99% reflectance at 1535nm wavelength and can achieve mechanical angle slew rates of over 500 rad/sec when switching the Er/Yb:Glass lasing cavity from pumping to lasing state. The design targeted higher efficiency, smaller size, and lower cost than the traditional Electro-Optical Q-Switch. Because pulse-on-demand capability is required, resonant mirrors cannot be used to achieve the needed performance. Instead, a fast point-to-point analog single-axis tilt actuator was designed with a custom-coated high reflectance (HR) mirror to withstand the high intra-cavity laser fluence levels. The mirror is bonded on top of the MEMS actuator in final assembly. A compact MEMS controller was further implemented with the capability of autonomous on-demand operation based on user-provided digital trigger. The controller is designed to receive an external 3V power supply and a digital trigger and it consumes ~90mW during the short switching cycle and ~10mW in standby mode. Module prototypes were tested in a laser cavity and demonstrated high quality laser pulses with duration of ~20ns and energy of over 3mJ.

Keywords: MEMS, MEMS Mirror, Q-Switch, Nd:YAG, Er:Glass, Er/Yb

## 1. INTRODUCTION

Q-switched lasers allow generation of short pulses with high peak powers [1]-[7] as required for many important applications across industries; marking, engraving, trimming, thin-film removal, drilling and cutting. Additional applications include medical and cosmetic treatments, laser range finding (LRF), laser detection and ranging (LADAR), communications, remote sensing, and laser designation, pointing and marking. In many of these applications, Er/Yb doped glass is the lasing medium of choice as it emits at the 1.5  $\mu\text{m}$  wavelength which enhances the laser system eye-safety [3]-[5].

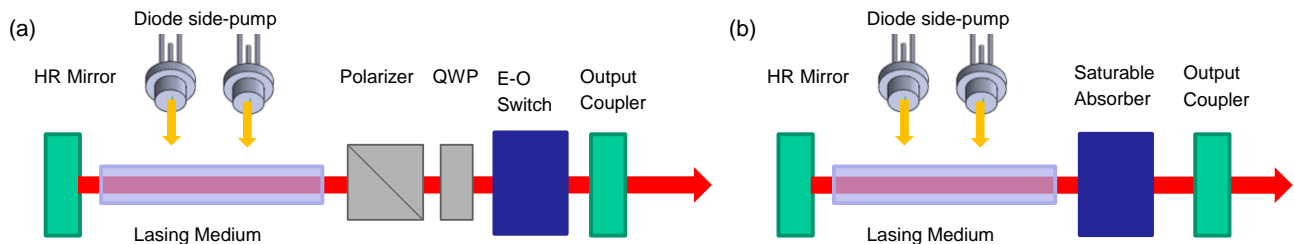


Figure 1. Schematic diagram of side-pumped Q-switched laser cavities (a) with active Electro-Optical Q-switch, (b) with passive Saturable Absorber Q-switch.

Figure 1 schematically shows two examples of Q-switched laser cavities. In one case of Fig. 1a, the cavity includes an electro-optic (EO) Q-switch and in the other case of Fig. 1b, the cavity includes a saturable absorber Q-switch. In both cases, in the off state the Q-switch serves to inhibit laser action either by blocking the light path, causing cavity misalignment by tilting one of the resonator mirrors, or reducing the reflectivity of one of the resonator mirrors. This enables optical pumping of significant energy into the lasing medium. A laser pulse is initiated when the Q-switch is

placed into low-loss condition; for a tilted-mirror mechanical Q-switch this occurs when the mirror angle is changed to achieve cavity resonance. Thus the accumulated energy is abruptly released with high peak power.

Although active electro-optic, acousto-optic, or passive saturable absorber Q-switches are most common, each has its own set of drawbacks. EO Q-switching is complex, relatively costly and needs a high voltage (2-3 kV) driver. It also requires an intra-cavity polarizer and a quarter-wave plate, with each additional component increasing optical losses, system complexity and cost. Although saturable absorber Q-switching is much simpler, it introduces significant intra-cavity loss due to unsaturated absorption, reducing laser efficiency. Passive Q-switching also does not allow adjustment of the laser output energy and causes significant pulse timing jitter. These deficiencies can be avoided with a mechanical Q-switch that rapidly rotates one of the Fabry-Perot resonator mirrors. Although rotating mirror devices are simple and inexpensive, they suffer from the tendency to emit multiple pulses and tend to be large, noisy, and require frequent maintenance. Pulse-on-demand generation requires nearly immediate control with highly repeatable and reliable mechanical action.

## 2. MEMS-BASED Q-SWITCH

Multiple research teams have investigated utilizing MEMS-actuated mirrors as Q-switches in laser cavities [6]-[10]. Namely, as described in Section 1, the fundamental requirements for a good Q-switch in a pulsed laser are to have high reflectance (mirror), and to have the ability to move into aligned position or out of aligned position (MEMS actuation). Therefore it can be natural to seek a solution in which a MEMS-actuated mirror is utilized as the Q-switching component in the pulsed laser. As depicted in Figure 2, the end HR mirror from Figure 1 could be replaced by a MEMS HR mirror at the end of the laser cavity. Because the mirror could actuate in and out of alignment with the cavity, multiple components from the E-O based switch (Figure 1a) or the saturable absorber based switch (Figure 1b) would be eliminated and optical efficiency significantly increased. In addition to that, if the requirements and performance can be met, MEMS-based Q-switches can be less costly because they can be batch fabricated with hundreds of devices on a single silicon wafer.

Lubeigt et al [8] have demonstrated that resonant MEMS mirrors can be employed as end mirrors in side-pumped laser cavities and achieved promising results while also encountering challenges with the heat generated by the considerable energy absorbed by the mirror. Bouyge et al [9] employed MEMS mirrors in doped fiber amplifiers and Peter et al. [10] in a Q-switched fiber laser. In all of the above referenced work, resonant actuation mirrors were used; these allow fast repetition rate (hundreds of Hz or several kHz) Q-switching, but not on-demand single-pulse firing. The pulse energies and peak powers achieved in these experiments were relatively low. In the case of resonant actuation, the required speed (slew rate) performance is achieved as a combination of large mechanical tilt angles of the mirror and fast resonant frequencies. To meet the requirement of on-demand single-pulse generation, the MEMS mirror Q-switch must be able to be triggered at an arbitrary time to follow the sequence of actuating from the “OFF” position (Figure 2a), used to build up laser inversion, to the “ON” position (Figure 2b) which initiates generation of the Q-switched pulse.

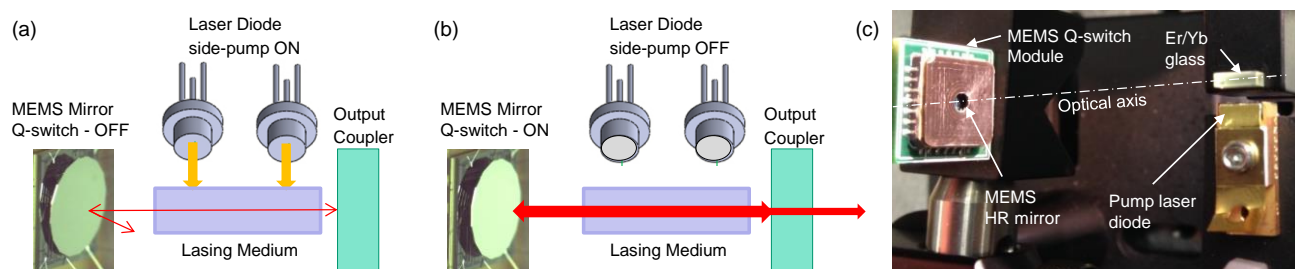


Figure 2. A side-pumped Q-switched laser cavity employing a MEMS mirror as the Q-switch and the cavity HR reflector: a) Schematic with the MEMS HR mirror in the “OFF” (or high loss) position and optical pumping ON, (b) schematic of the MEMS mirror in the “ON” position (low loss) with laser pulse generation, and (c) a photograph of a prototype Q-switched laser verifying the principles in the schematic with the proposed HR-coated MEMS mirror.

The focus of this project was to introduce a MEMS-based approach with the above-mentioned improvements compared to other Q-switch technology, while at the same time adding the advantage of offering full control of the switching sequence with on-demand pulse emission, at the push of a button. Targeting very low power consumption, competitive cost, and a highly compact volume would result in an excellent candidate for a variety of Er/Yb based lasers.

### 3. HIGH REFLECTIVITY COATED MIRROR

One of the most critical challenges in fabricating a MEMS Q-switch is achieving a low-mass mirror that has high reflectivity, is optically flat, and exhibits a high optical damage level needed for generation of high peak power laser pulses. For a lasers based on low gain Er/Yb glass, the optimum output coupler mirror reflectivity was found to be in the range of 90-92%. To avoid significant excess laser cavity loss, it is desirable to use a HR mirror with a reflectivity of >99.5%, where the 0.5% residual loss includes coating absorption, scattering, and any additional loss due to beam clipping by the mirror aperture. This mirror requirement can only be achieved with the use of multi-layer dielectric coatings, rather than the metal coatings that are used in the more common MEMS mirror applications.

In our initial experiments, MEMS Q-switches with Aluminum and Gold metal film mirrors were tested. Although these metal coatings withstood the long pulse laser operation corresponding to low peak powers, when Q-switched laser operation was initiated, they were quickly damaged at output pulse energies significantly below 1mJ. To withstand the >20J/cm<sup>2</sup> intra-cavity fluence calculated for a 3mJ, 20ns pulse with Gaussian beam 1/e<sup>2</sup> diameter of 0.8 mm, we transitioned to mirrors using a multi-layer dielectric coating with a reflectivity of >99.5%. The use of such mirror coatings in MEMS Q-switch, however, introduced a major challenge in maintaining good mirror flatness in the presence of mechanical stress induced by the coating on the thin, low-mass, Si mirror substrates. The thickness of a typical 1535nm HR coating can be as much as a hundred times more than the thickness of a metal film mirror coating. To assure good mirror flatness in the presence of stress-induced bending forces resulting from such a thick coating, the mirror substrate itself must become much thicker than the ~40μm typically used in MEMS mirrors. Even if this thickness is doubled at the expense of added inertia, the thick multi-layer dielectric coating would easily bend the substrate to a curvature too high for use in the laser resonator. Figure 3a schematically shows the simulated effect of a thick dielectric HR mirror coating with the typical compressive-stress when applied to a single side of a 100 μm thick Si wafer versus when applied to both sides of the wafer. Based on multiple experiments we found that applying the same coating, reproduced as closely as possible, on both sides of the Si wafer significantly reduced the mirror curvature. In order to consistently achieve a mirror curvature radius greater than 5m, we used 175-200μm thick Si substrates.

Regarding the underlying mirror substrate - in the project we experimented both with fused silica substrates and with silicon substrates. Overall, it was found that silicon is superior to glass as a substrate as the base substrate in mechanical and thermal performance and at the same time availability of thin high quality double-side polished silicon substrates was found to be much better. It is also understood that silicon could be micromachined more easily to create circular or other specific shapes and in that sense better suited for mass production. As already mentioned, to allow for coating on both sides of the wafer to compensate for any stress-induced curvature, double-side polished (DSP) wafers were utilized, in various thicknesses (Figure 3).

The process of fabricating the HR mirrors was therefore simplified as follows. DSP silicon wafers with high optical quality polishing on both sides are purchased from wafer suppliers and sent to optical coating houses for the HR coating. The HR coating is uniformly applied to both sides of the DSP wafer and the resulting reflectance is verified by measurement. Coated wafers are then diced down to 1.6mm x 1.6mm square mirror shapes which are thoroughly cleaned and dried. Those are then individually tested on a white light interferometer for flatness. Namely, our numerous tests found that only mirrors with >5m radius of curvature can result in high quality Q-switching performance and therefore only mirrors with those results pass this stage. Finally, those mirrors are ready for bonding into pre-assembled and pre-tested MEMS actuators as shown in Figure 3d. The assembly step itself is performed at a probe station with a simple pick and place tool and under microscope for achieving alignment into the center of the actuator. Bonding between the MEMS actuator and the coated silicon mirror is achieved with a tiny droplet of heat-curable adhesive.

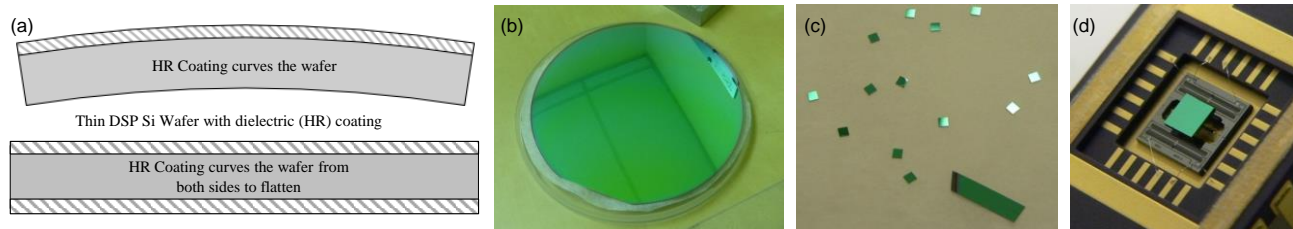


Figure 3. (a) Wafer curvature affected by single side HR coating vs. double side HR coatings. (b) A 4" diameter silicon wafer, HR-coated for 1535nm with >99% reflectance, (c) 1.6mm x 1.6mm diced square pieces of the wafer, ready for testing and assembly with MEMS actuators, (d) Photograph example of a single-axis MEMS actuator with an HR mirror square bonded onto the center stage.

#### 4. MEMS ACTUATOR FOR HIGH ANGULAR SLEW RATE

The MEMS actuator design was based on the 4-quadrant (two bi-directional axes) gimbal-less MEMS actuator technology utilized in a variety of MEMS mirror products [11]-[13]. The gimbal-less MEMS actuator technology based on vertical combdrive rotators [12] was specifically developed and continues to be utilized for analog tilt angle point-to-point optical beam steering technology and was therefore a good candidate for this specialized requirement. Furthermore, the pure single-crystal silicon construction of the gimbal-less MEMS results in high reliability and repeatability over time, temperatures, and other environmental factors in a simple, voltage driven open loop operation. The devices can be operated over a wide bandwidth from DC (maintain position) to several thousand Hertz. Such fast and broadband capability allows nearly arbitrary waveforms such as constant velocity scanning, and point-to-point step scanning etc. All-electrostatic design with <20pF total capacitance enables ultra-low operating power (<5 mW) even at the highest operating frequencies, which is ideal for battery operated laser devices. Compared to the large-scale galvanometer-based optical scanners, and even magnetic-based MEMS actuators, our devices require multiple orders of magnitude less driving power.

As mentioned above, the complete MEMS actuator is fabricated from single-crystal silicon, excellent material for such miniature flexing mechanical designs. It has nearly perfect elastic properties and has no long-term degradation, or plastic deformation, and is superior in long-term stability and repeatability compared to polysilicon and other materials. Single crystal Si is a fully elastic material; as the flexure undergoes deformation, the internal stress increases, but as the force causing the deformation is removed, the material returns elastically to its undeformed state. Such extremely repeatable elastic performance gives nearly infinite lifetime in terms of number of cycles and years of operation. This is only the case, however, if devices are constructed with no mechanical parts contacting, rubbing, latching, and designed to operate with flexural stresses at relatively low percentage of the theoretical stress failure limit. Our device designs follow these rules. The combdrive actuators, supporting shuttles and all of the flexing beams are made in one silicon layer. Design focuses on reducing any potential stress concentrating features and preventing any inadvertent contact between opposing fingers or flexures. Based on this, the devices can run 10s of billions of cycles without notable degradation.

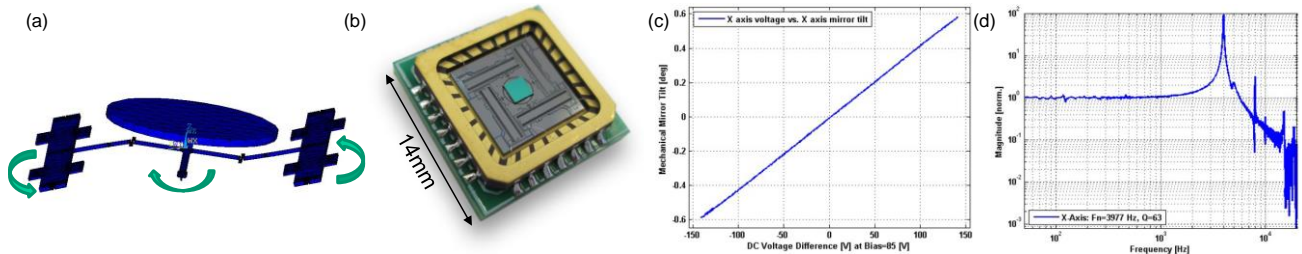


Figure 4. Latest Q-switch MEMS device design. (b) Photograph of a completed MEMS actuator with the HR mirror bonded in the middle. (c) Voltage vs. Angle - static response, (d) small signal frequency response.

To maximize simplicity and compactness, and to minimize power consumption, we have focused efforts on a single-axis architecture with bi-directional rotation capability. The single-axis design schematically shown in Figure 4a utilizes two electrostatic combdrive rotators working together to rotate the mirror in the middle about its underlying axis. There are essentially six suspending beams which support the complete structure and allow torsional bending / rotation. Each rotator has one supporting beam at each end, providing it with a rotation axis along its length. And the central shuttle beneath the mirror has one supporting beam at each end, providing it with the central rotation axis. This arrangement provides the structure with a high stiffness in lateral and vertical displacement directions while allowing the designer to tune the rotational stiffness according to the desired voltage-theta relationship.

During the design we performed extensive simulations of design variations to determine an optimal voltage vs. angle (V- $\theta$ ) relationship for the mirror actuator. The above described device design is highly flexible and could be varied to provide the mirror with e.g.  $+2^\circ$  of mechanical rotation or all the way down to  $+0.4^\circ$ . From the point of view of the application requirement for laser cavity loss modulation (Q-switching), as little as  $0.1^\circ$  of mechanical movement is sufficient. Nevertheless a significant design effort was needed to determine the target angle for the device because the combination of point-to-point angle capability and speed determines the angular slew rate performance which is critical for good pulse forming. Naturally, for each such V- $\theta$  design variation (by varying stiffnesses of supporting beams,) a different speed of rotation is found. Therefore a complete simulation cycle for a design variation must include static V- $\theta$  analysis as well as modal / speed analysis. First step is typically to analytically determine the V- $\theta$  gain from the combdrive design and mechanical beam stiffnesses. Then, the structure is simulated in a finite element analysis to find its

natural modes and specifically to determine its first rotational resonance which dominates the response as seen in Figure 4d. From the V- $\theta$  relationship (e.g. Figure 4c ) and the rotational resonant mode (as seen in the real device measurement in Figure 4d), a simple linear model is constructed. This model is then simulated with various step driving / excitation waveforms and the resulting angular slew rate and the amount of residual ringing is observed.

Finally, it was decided that the MEMS actuators should be designed and fabricated to achieve a tilt range of approx.  $-0.5^\circ$  to  $+0.5^\circ$  when excited with voltage differences of up to 145V. Several devices were packaged and tested and it was found that the fabricated devices matched the design very closely. A measured static V- $\theta$  graph of a typical device is seen in Figure 4c. This mechanical angle measurement was performed by applying 85V bias voltage to all actuator segments and then varying the difference between +angle rotation section and -angle rotation section from -145V to +145V. These small angle devices are supported by very stiff silicon beams and therefore despite the thick and relatively large HR mirrors, they resulted in very high first resonant frequency of nearly 4kHz as seen in Figure 4d.

### 5. DRIVING METHODOLOGY AND COMPACT MEMS DRIVER DESIGN

The driving methodology for the MEMS mirror should satisfy the main requirement of on-demand pulse emission, but also result in a very compact, low cost, and very low power consuming driver. The operation sequence with the power saving in mind was arranged as follows: once a user requests a laser pulse by depressing a trigger, the Q-switch module is enabled which moves the MEMS mirror into OFF position misaligned to the cavity (Figure 2a), thereby allowing optical pumping. Then, after a programmable amount of time (e.g.  $\sim 5$  ms), the mirror quickly moves to a new angle, and during that movement briefly aligns with the cavity optical axis (Figure 2b) to establish a high quality factor (or “high-Q”) resonant condition which allows the medium to release its energy. The result is a single, very high peak power laser pulse with a duration on the order of tens of nanoseconds and energy in the range of several milli-Joules. The Q-switch module is subsequently disabled back into standby mode for ultra-low power consumption.

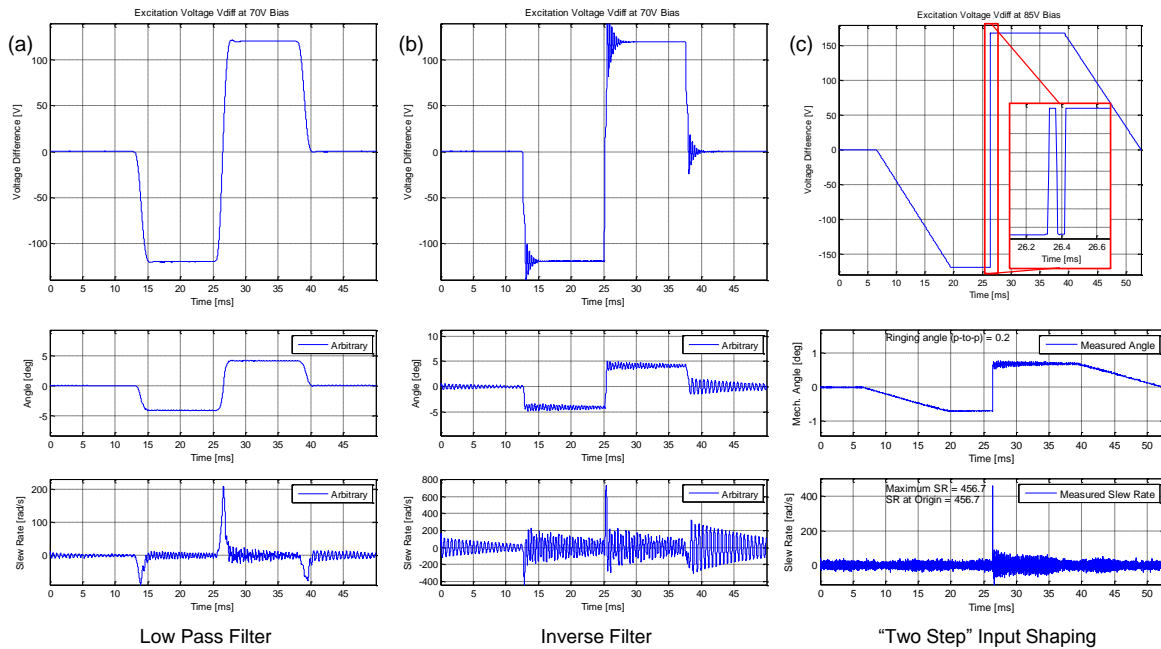


Figure 5. Measured drive waveforms and resulting mechanical tilt data of a single-axis actuator with a square-shaped 1.6mm HR mirror. Three drive methods are compared as follows: a) Low pass filter method resulted in minimum ringing and  $\sim 210$  rads/sec tilt angle slew rate. b) Inverse system filter method resulted in larger but acceptable ringing and  $\sim 700$  rads/sec, and c) Two-step input shaping method resulted in some ringing and slew rate of 456.7 rads/sec.

We experimentally determined that for the 25-50 mm long Er/Yb laser resonators, generation of an efficient solitary Q-switched pulse required the HR mirror to slew through the alignment position at  $>200$  rad/sec mechanical rotation rate. Slower slew rates typically caused the Q-switched pulse to break up into multiple, lower energy pulses. This is a very high speed of rotation relative to the large mirror inertia and requires an aggressive driving methodology. It can be surmised that the fastest slew rate response from such a micromechanical device could be obtained by applying a sharp

step input voltage. The result of course is very fast movement toward the new position, however followed by large amplitude oscillations (ringing) which actually pass through the cavity alignment position again and again, resulting in uncontrolled laser outputs. Thus, the step input waveform must be carefully shaped to result in fast slewing but with minimal overshoot and ringing. As seen in Figure 5 we investigated multiple input shaping methodologies such as low pass filtering, inverse filtering, and a “two step” input shaping. Low pass filtering is often used with more typical MEMS mirror applications and here the goal is to suppress the mirror resonance by reducing the available drive waveform bandwidth. The step waveform is filtered in software with a 2<sup>nd</sup> order Bessel filter with the cut-off frequency at  $1/3 * f_n$ , where  $f_n$  is the resonance. The low pass filtered method had the slowest resulting slew rate (200 rad/sec, Figure 5a), but the also the least overshoot and ringing. In order to increase the slew rate, an inverse filter [13] was used which achieved the highest slew rates ( $>700$  rad/sec, Figure 5b). This is again a software filtered step function but with a filter specifically designed to invert the system model and extend the bandwidth to about  $2 * f_n$ . The inverse filter created the most overshoot and ringing of the three driving schemes, with the device was ringing somewhat above our target 10% margin. This could however be tuned by slightly reducing the bandwidth.

While the inverse filter method gives excellent speed performance, it was deemed too complex when considering the target compactness of the MEMS mirror driver. We investigated further to find schemes which would allow us to entirely remove the need for a DAC in the driver and any kind of buffer / memory for storing waveforms. Therefore we experimented with digital-only waveforms (full positive voltage difference or full negative voltage difference) but with controlled timing to reduce ringing, akin to posicast and other input shaping feed-forward controls [14][15]. Figure 5c shows the driving waveform where the step function is composed of a positive step, then a quick negative step, and then the final positive step. The duration of the first positive and negative step can be varied to get the least overshoot and ringing and to control slew rate. Various Simulink simulations provided the optimal duration of each of the two pulses to be  $\sim 0.17 / f_n$ , although a variation of  $\pm 10\%$  in  $f_n$  did not significantly degrade performance. As an additional control-knob, by adjusting the high voltage supply, the two-step input waveform can drive the MEMS device from slew rates of  $\sim 200$  rad/sec up to  $\sim 500$  rad/sec. This two-step method was chosen for the driver implementation due to its highest simplicity.

## 6. TEST SETUP AND RESULTS

Each assembled MEMS device is first tested for static and dynamic performance with a general MEMS mirror test setup, i.e. without the use of the specialized driver described above. Here a calibrated 2D position sensitive device (PSD) is first used to measure the device’s static voltage difference vs. angle performance, similar to characterization of any 4-quadrant MEMS mirror [11]. Figure 4c shows that the most recent design achieves approximately  $-0.5^\circ$  to  $+0.5^\circ$  of mechanical tilt when actuated from 0V to 170V difference about the 85V bias with a highly linear angle to voltage relationship. Then, the device’s frequency response is measured by applying noise excitation. The typical resulting response in Figure 4d shows that there is a very uniform response from DC to  $\sim 3$ kHz and a strong resonance at 3.9kHz.

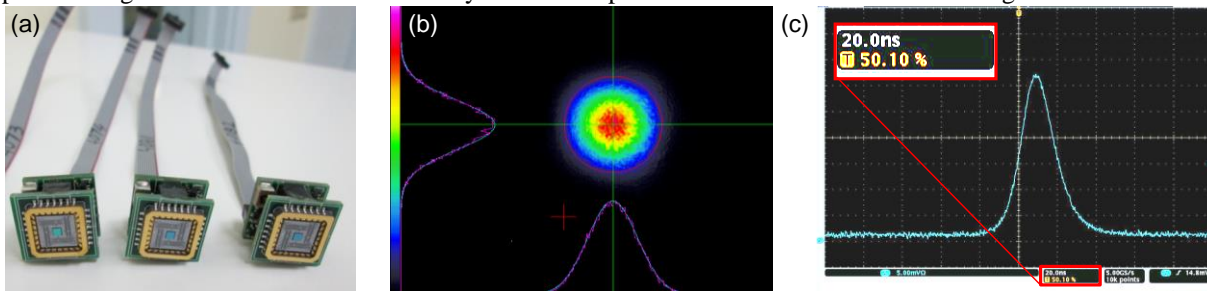


Figure 6. (a) Fully assembled Q-Switch MEMS modules, (b) laser beam far field intensity profile, (c) Q-switched pulse shape, 20 ns FWHM.

After the Q-switch MEMS device passes the above tests, the compact MEMS driver is added, and the completed module goes through the angular slew rate characterization. The Q-switch module, using a visible laser, faces the calibrated wall used in the datasheet process, and scans across multiple photo-transistors on the wall when a trigger is issued to perform the Q-switch operation. The photo-transistors are placed a known distance apart, and the response of the photo-transistors (Figure 6a) is measured on an oscilloscope. The time between the two pulses measured, the distance between the two photo-transistors, and the distance from the Q-switch to the photo-transistors is used to calculate the mechanical angle slew-rate of the Q-Switch. The slew-rate can be adjusted on the compact MEMS driver by increasing or decreasing the high voltage supply to the MEMS device. Once the desired slew-rate of  $>250$  rad/sec is reached, the module may be packaged into its final housing, and is ready to be placed into an Er/Yb laser cavity.

The final tests in a laser cavity can test the HR-mirror to confirm the device can handle the power required in a given application. The cavity setup includes (Figure 2c), a 4 cm long resonator cavity consisting of the MEMS Q-switch, a 940 nm side-pumping laser diode bar, and an Er/Yb doped glass gain element. The R=90-92% laser output coupler mirror was directly deposited onto the 1.5mm x 3mm end-face of the Er/Yb glass element, whereas the opposite end face was AR-coated. Q-switched pulses exceeding 3mJ were generated with an optical to optical efficiency of >2%. The pump laser, generating 50 W peak power, was on for 3ms for each pulse; the laser was run at a pulse repetition frequency rate of 1 Hz. To increase the cross-section of the pumped volume, the diode bar was displaced by 1.5 mm from the side-wall of the Er/Yb glass. The Gaussian near-field had a  $1/e^2$  diameter of 0.8 mm, and the beam divergence was 2.5 mRad (Figure 6b). The Q-switched pulse length was 20ns FWHM (Figure 6c), no mirror damage was observed despite the high intra-cavity energy fluence of  $\sim 20 \text{ J/cm}^2$ .

## 7. CONCLUSIONS

A Si-based fast-scanning, single-axis micro-electro-mechanical system (MEMS) mirror for Q-switching of high peak power lasers is demonstrated. The MEMS device uses a dielectric-coated Si mirror to avoid optical damage, allowing intra-cavity energy fluences of  $>20 \text{ J/cm}^2$ . Mirror rotation slew rates of  $>500 \text{ rad/sec}$  were demonstrated with a 1.6mm x 1.6mm area mirror. A tested MEMS Q-switched Er/Yb glass laser generated 3mJ, 20ns pulses at 1.5  $\mu\text{m}$  wavelength, with a near-diffraction-limited output beam.

## 8. REFERENCES

- [1] W. Koechner. "Solid-State Laser Engineering", sixth edition. Springer science + business Media Inc. 2006.
- [2] J. Taboada, *et al.* "100-megawatt Q-switched Er-glass laser", Proc. SPIE 6100, Solid State Lasers XV: Technology and Devices, 61000B, Feb. 2006.
- [3] J. E. Nettleton, B. W. Schilling, D. N. Barr, and J. S. Lei, "Monoblock laser for a low-cost, eyesafe, microlaser range finder", Applied Optics, vol. 39, no. 15, May 2000.
- [4] Lew Goldberg, John Nettleton, Brad Schilling, Ward Trussel and Alan Hays, "Compact laser sources for laser designation, ranging and active imaging", Proc. SPIE 6552, 65520G (2007).
- [5] J. Hecht, "PHOTONICS FRONTIERS: EYE-SAFE LASERS – Retina-safe wavelengths benefit open-air applications", LaserFocusWorld, March 1, 2008.
- [6] L.A Spinelli, A. Caprara, J.H. Jerman, "Low Power Q-Switched Solid State Lasers," US Patent 2007/0268950, Nov. 22, 2007.
- [7] J. Nettleton, D. N. Barr, MEMS Q-Switched Monoblock Laser, US Patent 2013/0044769, Feb. 21, 2013.
- [8] W. Lubeigt, J. Gomes, G. Brown, A. Kelly, V. Savitski, D. Uttamchandani, and D. Burns, "Control of solid-state lasers using intra-cavity MEMS micromirror", Optics Express, Vol. 19, No. 3, Jan. 2011, pp. 2456-2465.
- [9] D. Bouyge *et al.*, "Integration of Micro-Electro-Mechanical Deformable Mirrors in Doped Fiber Amplifiers", Dans Symposium on Design, Test, Integration and Packaging of MEMS/MOEMS - DTIP 2006, Stresa, Italy (2006).
- [10] Y.-A. Peter, *et al.*, "Q-switched fiber laser using a torsional micro-mirror", Advanced Applications of Lasers in Materials Processing, IEEE/LEOS 1996 Summer Topical Meetings, 5-9 Aug. 1996.
- [11] [www.mirrorcletech.com/support.html](http://www.mirrorcletech.com/support.html)
- [12] V. Milanović, D. T. McCormick, G. Matus, "Gimbal-less Monolithic Silicon Actuators For Tip-Tilt-Piston Micromirror Applications," IEEE J. of Select Topics in Quantum Electronics, Vol. 10, no. 3, May-June 2004.
- [13] V. Milanović, K. Castelino, "Sub-100  $\mu\text{s}$  Settling Time and Low Voltage Operation for Gimbal-less Two-Axis Scanners," 2005 IEEE/LEOS Optical MEMS and Their Applications, Oulu, Finland, Aug. 2005, pp. 127-128.
- [14] J. Y. Hung, "Posicast Control Past and Present," IEEE Multidisciplinary Engineering Education Magazine, vol. 2, no. 1, March 2007.
- [15] N. C. Singer, W. P. Seering, "Preshaping Command Inputs to Reduce System Vibration," J. Dyn. Sys., Meas. Control, 112, pp. 76–82, 1990.
- [16] M. Fabert, *et al.*, "Ytterbium-doped Fibre Laser Q-Switched by a Cantilever-Type Micro-Mirror," OPTICS EXPRESS, Vol. 16, No. 26, Dec. 2008, pp. 22064-22071.
- [17] D. Sabourdy, *et al.*, "Novel Active Q-Switched Fiber Laser Based on Electrostatically Actuated Micro-Mirror System," Optics Express, Vol. 14, No. 9, May 2006, pp. 3917-3922.